RESEARCH REPORTS
Biomaterials & Bioengineering

M.K. Pugach[1], J. Strother[2], C.L. Darling[1], D. Fried[1], S.A. Gansky[3], S.J. Marshall[1], and G.W. Marshall[1]*

[1]Department of Preventive and Restorative Dental Sciences, University of California, 707 Parnassus Ave. Box 0758, Dentistry 2246, San Francisco, CA 94143-0758, USA; [2]Naval School of Health Sciences, 2310 Craven St., Bldg. 3232, San Diego, CA 92136, USA; and [3]Department of Preventive and Restorative Dental Sciences, University of California, 3333 California St., Laurel Heights 495C3 Box 1361, San Francisco, CA 94143-1361, USA; *corresponding author, gw.marshall@ucsf.edu

J Dent Res 88(1):71-76, January, 2009

Dentin Caries Zones: Mineral, Structure, and Properties

ABSTRACT

Caries Detector staining reveals 4 zones in dentin containing caries lesions, but characteristics of each zone are not well-defined. We therefore investigated the physical and microstructural properties of carious dentin in the 4 different zones to determine important differences revealed by Caries Detector staining. Six arrested dentin caries lesions and 2 normal controls were Caries-Detector-stained, each zone (pink, light pink, transparent, apparently normal) being analyzed by atomic force microscopy (AFM) imaging for microstructure, by AFM nano-indentation for mechanical properties, and by transverse digital microradiography (TMR) for mineral content. Microstructure changes, and nanomechanical properties and mineral content significantly decreased across zones. Hydrated elastic modulus and mineral content from normal dentin to pink Caries-Detector-stained dentin ranged from 19.5 [10.6-25.3] GPa to 1.6 [0.0-5.0] GPa and from 42.9 [39.8-44.6] vol% to 12.4 [9.1-14.2] vol%, respectively. Even the most demineralized pink zone contained considerable residual mineral.

KEY WORDS: dentin, caries, mineral, mechanical properties, atomic force microscopy

INTRODUCTION

Current management of caries involves non-invasive techniques and maximum conservation of tooth structure. Differentiation between heavily infected outer carious dentin and demineralized, affected inner dentin reduces the risk of pulp exposure, maximizing reparative potential (McComb, 2000). Different layers of dentin caries lesions have been classified by clinical and laboratory techniques (Fusayama and Terachima, 1972; Anderson *et al.*, 1985), but recommendations may conflict or overlap. Therefore, it is essential that the nature of and variations in such lesions be understood.

Caries-staining products have been developed (Fusayama and Terachima, 1972) to assist clinicians during caries removal. Although the biochemical principle of staining carious dentin has been reported (Ohgushi and Fusayama, 1975; Kuboki *et al.*, 1977; Kuboki *et al.*, 1983), it remains unclear what characteristics of the lesion are stained, or how staining is related to microstructural features of various caries lesion zones. Not all stainable dentin is infected (Kidd *et al.*, 1993), but the absence of stain does not ensure bacterial elimination (Anderson *et al.*, 1985).

Caries staining characteristics have been described as pink, light pink, transparent, and apparently normal dentin, and nano-indentation properties of moderately active and arrested caries lesions have been compared (Zheng *et al.*, 2003). Nanohardness values for intertubular dentin increased from the pink zone to the apparently normal dentin layer (outer to inner). In another study, mechanical properties across dentin caries lesions decreased as the lesion surface was approached (Angker *et al.*, 2004b).

Hydration and dehydration affect dentin mechanical properties, especially demineralized dentin (Kinney *et al.*, 1993, 1996; Marshall, 1993). Therefore, properties measured under hydrated conditions provide more realistic estimates of those found *in vivo* (Marshall *et al.*, 2001).

The hypothesis for this study was that Caries Detector staining allows for the discrimination of carious zones with distinct microstructural characteristics, mechanical properties, and mineral contents. We investigated the zones revealed by Caries Detector staining in arrested caries lesions. We related these zones to their microstructural features as determined by atomic force microscopy (AFM), nanomechanical properties as determined by AFM nano-indentation, and mineral concentration.

MATERIALS & METHODS

Tooth Selection and Sample Preparation

Teeth were collected following protocols approved by the UCSF Committee on Human Research, and informed consent was obtained for the use of human tissues. Eight freshly extracted, unrestored third molars (6 carious, 2 non-carious controls), obtained from research participants requiring extractions for dental treatment, were sterilized by gamma radiation (White *et al.*, 1994), then stored in Hanks' balanced salt solution at 4ºC (Habelitz *et al.*, 2002). After the tooth was longitudinally sectioned

DOI: 10.1177/0022034508327552

Received November 14, 2007; Last revision September 11, 2008; Accepted September 24, 2008

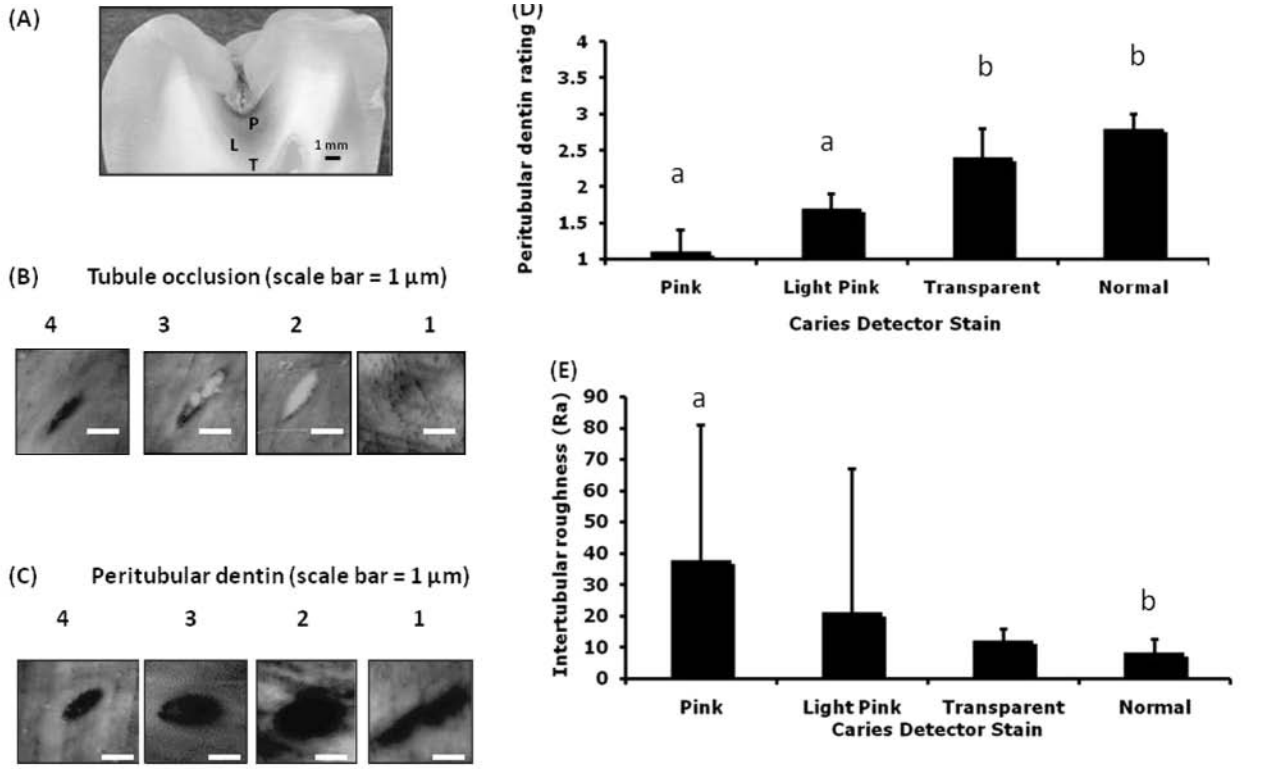

Figure 1. Carious morphological features. **(a)** Representative section through an arrested dentin caries lesion showing each Caries Detector zone, pink (P), light pink (L), transparent (T), and apparently normal (N). AFM height images (n = 61) showing examples of **(b)** tubule occlusion (TO) (scale bar = 1 µm), 4 = open, 3 = partial, 2 = closed, 1 = covered; **(c)** peritubular dentin (PT) (scale bar = 1 µm), 4 = complete, 3 = partial, 2 = none, 1 = distorted (images 30 x 30 µm); **(d)** PT rating means for each CD stain (n = 8) with 95% confidence boundaries indicated; **(e)** intertubular roughness (R_a) measurement means of CD stain zones (n = 8), with 95% confidence boundaries indicated. (Different letters a, b indicate non-overlapping confidence bounds corresponding to significant differences; error bars show 95% confidence bounds.)

through the lesion center by means of a water-cooled saw (Isomet low-speed saw; Buehler, Lake Bluff, IL, USA), a tooth with an obvious lesion appearing to extend 50-75% through the dentin thickness was eligible for the lesion group (Zheng *et al.*, 2003). Longitudinal sections (2 mm thick) through the center of the lesion were further sectioned from occlusal surface to pulp chamber to produce 2 x 2 x ~8 mm sticks. Similar sticks were sectioned from normal dentin controls. The surface was polished with waterproof SiC papers, under running water, with grit sizes of 600 to 1200, and 1- and 0.25-µm diamond pastes. This prepared surface was stained by Caries Detector (Kuraray, Osaka, Japan). Six lesions exhibiting apparently arrested caries (discolored, firm consistency, lightly Caries-Detector-stained) were identified for the lesion group. Digital images of each prepared surface were recorded.

Classification of Dentin Caries Lesion Zones

Four zones were identified in the lesions, based on their optical appearance and degree of staining: pink, light pink, transparent, and apparently normal. A representative section through an arrested dentin caries lesion can be seen (Fig. 1A), showing each Caries-Detector-stained zone, before being further sectioned into sticks.

Carious Dentin Microstructure Analysis by AFM

Using the Triboscope (Hysitron, Minneapolis, MN, USA) indenter tip of the AFM (Nanoscope III, Digital Instruments, Santa Barbara, CA, USA), we took a 30 µm by 30 µm AFM image of each area before and after nano-indentation, to examine the dentin microstructure in each area. Microstructural criteria included tubule occlusion, peritubular dentin, and intertubular roughness.

For each AFM image, the total number of tubules was determined. To assess tubule occlusion, we gave each tubule a rating between 4 (open) and 1 (completely closed) (Fig. 1B). For peritubular dentin assessment, the ratings were 4 (complete peritubular dentin surrounding the lumen), 3 (lumen partially surrounded), 2 (no peritubular dentin, but tubule shape was undistorted), and 1 (if no peritubular dentin and the tubule had a distorted shape) (Fig. 1C). This peritubular dentin rating system accounted for the difference between a loss of peritubular dentin in the initial stages of demineralization and the tubule distortion characteristic of more advanced demineralization caused by dentin caries. Average ratings for tubule occlusion and peritubular dentin were determined for each AFM image. These ratings were then related to additional physical and mechanical properties and Caries Detector stain.

Table. Means According to Caries Detector Stain*

Feature	Caries Detector Stain			
	Normal	Transparent	Light Pink	Pink
Peritubular dentin rating	2.8 [2.7-3.0][a]	2.4 [2.1-2.8][a]	1.7 [1.6-1.9][b]	1.1 [1.0-1.3][b]
Tubule occlusion rating	3.3 [3.1-3.4][a]	2.9 [2.6-3.2]	2.6 [2.4-2.8][b]	2.1 [1.6-2.7][b]
Intertubular R_a (nm)	8.3 [4.6-12.7][a]	12.3 [8.8-16.2]	21.1 [6.7-67.0]	37.8 [15.5-80.9][b]
Elastic modulus dry (GPa)	23.8 [21.8-26.4]	18.1 [11.3-25.3]	17.1 [12.0-22.8]	11.4 [0.1-23.2]
Elastic modulus wet (GPa)	19.5 [10.6-25.3][a]	14.4 [1.2-26.7]	9.8 [2.3-17.8]	1.6 [0.0-5.0][b]
Hardness dry (GPa)	1.63 [0.95-2.49][a]	0.65 [0.24-1.25]	0.52 [0.30-0.88][b]	0.31 [0.01-0.50][b]
Hardness wet (GPa)	0.87 [0.10-1.20][a]	0.58 [0.00-1.00]	0.63 [0.05-1.10]	0.05 [0.00-0.10][b]
Mineral content (vol%)	42.9 [39.8-44.6][a]	37.0 [36.9-37.1][a]	26.2 [19.8-32.3][c]	12.4 [9.1-14.2][d]

* Characterization criteria means (n = 8). Bootstrap mean and 95% confidence boundaries are shown. Different letters a, b, c, d indicate non-overlapping confidence bounds corresponding to significant differences between stains.

Intertubular surface roughness (root mean square roughness, R_a) of the peaks and valleys of the analyzed area was measured with the roughness analysis option from AFM software (Nanoscope III, version 5.12r3, Digital Instruments, Santa Barbara, CA, USA) (Oliveira *et al*., 2003). Three 5 μm by 5 μm images of intertubular dentin were chosen from the same images as used for tubule occlusion and peritubular dentin analyses.

Measurement of Reduced Elastic Modulus and Hardness

Reduced elastic modulus and hardness along the stick used for the microstructural evaluation were determined by an AFM modified with a Triboscope nano-indenter (Hysitron, Minneapolis, MN, USA), as previously described (Balooch *et al.*, 1998; Marshall *et al*., 2001). Nano-indentations were performed with a Berkovich diamond tip, both dry and in a liquid cell filled with de-ionized water, with a trapezoidal force profile with peak loads between 50 μN and 500 μN, and three-second indentation times. Each indentation yielded a load-deformation curve, from which the reduced elastic modulus, E, and hardness, H, were determined according to the following equations (Doerner and Nix, 1986):

$$E = \sqrt{\pi}/2\sqrt{a} \bullet S$$
$$H = F_{max}/a$$

where S represents the slope of the unloading curve based on the method of Oliver and Pharr (1992), *a* is the indentation contact area, and F_{max} is the maximum force. Calibration used a silica standard as previously described (Marshall *et al*., 2004). Five indentations were made in intertubular dentin at ~ 350-μm intervals along a line from near the pulp chamber to the carious occlusal surface. We collected AFM images before and after indentations to ensure that they were uniform, well-defined, and within intertubular dentin.

Measurement of Mineral Concentration

We used a custom-built digital transverse microradiography (TMR) system to measure mineral concentration in the dentin caries lesions (sections approx. 200 μm thick), and the equipment and technique have been described previously (Darling *et al*., 2006). The vol% mineral of each section was determined with a calibration curve of x-ray intensity *vs*. sample thickness created with sound enamel sections of 86.3 ± 1.9% vol% mineral, varying from 50 to 300 μm in thickness. The calibration curve was validated *via* comparison with cross-sectional microhardness measurements. The vol% mineral determined by microradiography for section thicknesses ranging from 50 to 300 μm was highly correlated with the vol% mineral determined by microhardness, $r^2 = 0.99$.

Statistical Analysis

We calculated means and 95% confidence intervals of each property (R_a, modulus, hardness, and vol% mineral) for each zone with a bootstrap sampling approach, stratifying on sample (selecting one measurement *per* zone *per* sample with replacement, calculating the mean, repeating 20,000 times, and determining the 5% and 95% bounds). We used Pearson's correlation coefficient (r) to assess the relationship of the properties (elastic modulus and hardness) with vol% mineral, with Spearman's rank (r_s) for ordinal data to assess the relationship of the properties (R_a, elastic modulus, hardness, and vol% mineral) with stain (zone). We assessed the relationship of peritubular dentin and tubule occlusion with Caries Detector stain with r_s, using a bootstrap procedure to select one tubule *per* stick and calculating r_s; this was repeated 20,000 times, and the distribution of r_s was determined with the mean and 5% and 95% bounds reported.

RESULTS

As expected, with increasing levels of demineralization, peritubular dentin rating, mechanical properties, and mineral content decreased (Table). Peritubular dentin rating varied significantly according to Caries Detector stain (Table, Fig. 1D). The correlation coefficient between peritubular dentin and Caries Detector stain was $r_s = 0.58$ (bootstrap 95% CI, 0.20, 0.82), indicating a significant association, and that between tubule occlusion and Caries Detector stain was 0.36 (bootstrap

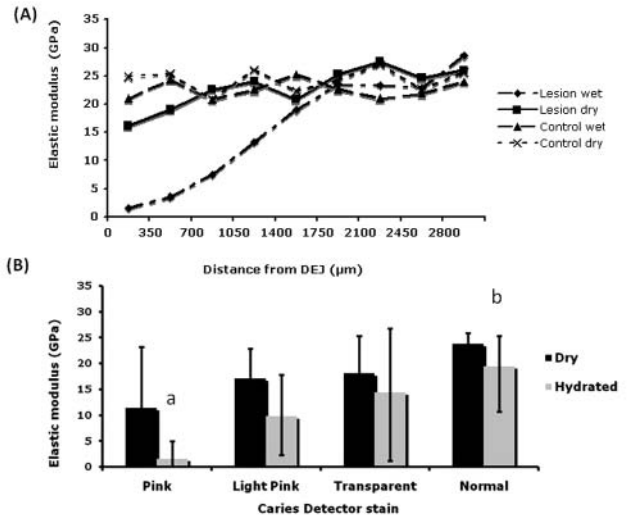

Figure 2. Nanomechanical properties of dentin caries lesions—AFM nano-indentation in hydrated and dry conditions. (**a**) Elastic modulus (E) in GPa of 1 lesion, under hydrated and dry conditions, and control (normal dentin). (**b**) E for each CD stain (n = 8) (Different letters a, b indicate non-overlapping confidence bounds corresponding to significant differences; error bars show 95% confidence bounds.)

95% CI, -0.09, 0.72), which was not significant. Mean intertubular R_a of the pink zone was significantly greater than that in the normal zone, as indicated by the non-overlapping confidence bounds (Table, Fig. 1E).

A typical elastic modulus profile of normal control dentin and a dentin caries lesion, along lines starting 3 mm below the DEJ, shows the decreased values in the demineralized zones (Fig. 2A). Dry modulus values were significantly correlated with the ordinal Caries Detector stain (normal, transparent, and light pink) ($r_s = 0.59$; bootstrap 95% CI, 0.12, 0.91) (Fig. 2B). Hydrated elastic modulus values were significantly less in pink than in normal, as indicated by non-overlapping 95% CIs (Fig. 2B). Hardness values are shown in the Table.

A microradiograph (Fig. 3A) from a representative dentin caries lesion with a vol% mineral line profile (Fig. 3B) through the lesion center shows mineral variations across the lesion. Vol% mineral differed significantly between Caries Detector stain zones, as indicated by non-overlapping bootstrap 95% CIs (Fig. 3C). Mineral content was significantly correlated with dry elastic modulus (r = 0.71; bootstrap 95% CI, 0.20, 1.00).

DISCUSSION

Previous studies have suggested that mechanical properties of a calcified tissue are associated with mineral content (Featherstone *et al.*, 1983; Arends and ten Bosch, 1992; Kodaka *et al*., 1992; Kinney *et al*., 1996; Angker *et al.,* 2004b). It has been reported that mechanical properties are significantly affected by wet or dry testing conditions (Angker *et al*., 2004a). In our study, elastic modulus of hydrated dentin could better distinguish between normal and pink stains than could dry nano-indentation, perhaps because the dentin was hydrated when it was Caries-Detector-stained. Hardness of both wet and dry dentin showed significant differences between normal and pink stain. Interestingly, dry nano-indentation measurements correlated better with Caries Detector stain, perhaps because of less variability.

A biochemical mechanism has been suggested for the stainability of carious dentin based on the remaining collagen that has been demineralized by cariogenic acids. The inner layer of carious dentin that stains most dramatically (pink zone) has decreased cross-links (Kuboki *et al*., 1977), allowing the stain to penetrate more efficiently. Furthermore, in one study, collagen was stainable only when demineralized by a cariogenic acid, which may indicate bacterial involvement in Caries Detector stainability (Kuboki *et al*., 1983), although there is disagreement about the correlation between stain and level of bacterial infection (Kidd *et al.,* 1993; Zacharia and Munshi, 1995). Our data are consistent with the idea that altered collagen cross-linking may contribute to increased stainability of the pink zone, and decreased mechanical properties. However, the exposure to cariogenic acids of the pink zone may simply remove more mineral, causing increased porosity, and hence increased stainability.

In this study, the Caries Detector stain sometimes gave false-positives in normal dentin near the pulp chamber, as well as false-negatives in slightly demineralized dentin that had not become porous enough to pick up the stain. These discrepancies agree with a previous report (McComb, 2000). The inconsistency of carious dentin staining could result from increased or decreased porosity, unrelated to mechanical properties, collagen structure, or microstructure, but instead caused by variations in tubule density.

Intertubular dentin modulus is a major determinant of overall elastic properties of dentin, and there is minimal contribution from the peritubular dentin properties (Kinney *et al*., 1996). Nano-indentations were made in intertubular dentin for accurate assessment of the mechanical properties of bulk dentin. However, the presence or absence of peritubular dentin is also important, since its dissolution is an early microstructural indicator of demineralization (Marshall *et al.*, 1998). Likewise, tubule occlusion by mineral deposits due to demineralization/remineralization cycles during the caries process (ten Cate *et al.*, 1988; Featherstone *et al.*, 1990; Featherstone, 2004) is an indicator of transparent dentin formation (Fusayama, 1991). Therefore, we analyzed AFM images from the nano-indented areas and rated each tubule for peritubular dentin and tubule occlusion. While peritubular ratings were significantly related to Caries Detector stain, tubule occlusion was not. Tubule occlusion was most apparent in transparent dentin, leading to its transparent optical appearance. While tubule coverage and distortion were observed in Caries-Detector-stained dentin, these tubules were not filled, but had loosely attached mineral or organic material.

Our study showed that when the dentin was stained by the Caries Detector, peritubular dentin disappeared, perhaps because the lack of peritubular dentin widened the tubules and intertubular dentin had been partially demineralized and was more porous. While peritubular dentin ratings were a good indicator of demineralization, they could not distinguish between partially demineralized (light pink) dentin and the more demineralized pink zone. Intertubular roughness (R_a)

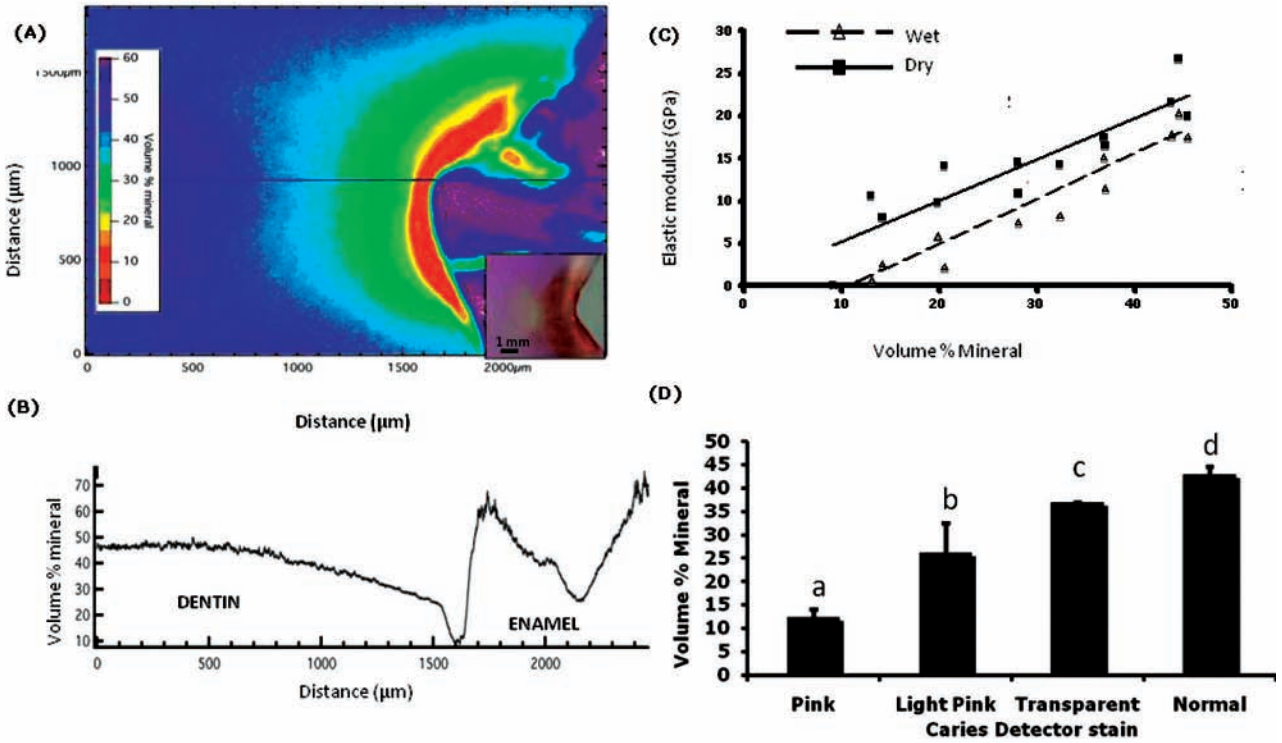

Figure 3. Digital transverse microradiography (TMR). (**a**) Vol% mineral color gradient TMR image showing a representative dentin caries lesion; inset shows corresponding CD-stained lesion. (**b**) Line profile showing vol% mineral along the line shown in (**a**), *vs*. distance in µm along lesion from above pulp to just above DEJ; (**c**) mineral content *vs*. E hydrated and dry (n = 8) [correlation (r) significant for E dry, $p < 0.05$]; and (**d**) vol% mineral averages by CD stain (n = 8). (Different letters a, b, c, d indicate non-overlapping confidence bounds corresponding to significant differences; error bars show 95% confidence bounds.)

measurements with AFM showed that R_a could also distinguish between normal and pink zones.

Caries Detector stain may not differentiate remineralizable demineralized dentin from that which should be removed. Thus, a greater understanding of the Caries Detector staining process is needed to improve its clinical utility. This study emphasized the importance of measuring dentin properties in hydrated conditions. Dry measurements of modulus or hardness may result in misleadingly high values in the more demineralized zones, but may produce less variable measures.

A significant finding of this study is that the most demineralized (pink) zone of these dentin caries lesions contained about 25% of the mineral of normal dentin. Previous studies of bone have shown that the mineral phase is partitioned between intrafibrillar mineral and extrafibrillar mineral within the spaces separating the fibrils (Landis *et al*., 1996). Extrafibrillar mineral makes up as much as 75% of the total mineral (Bonar *et al*., 1985), leaving 25% intrafibrillar mineral. Therefore, the pink zone may contain remaining intrafibrillar mineral, which may have important consequences for remineralization and the restoration of mechanical properties (Kinney *et al*., 2003).

In conclusion, the characterization of Caries-Detector-stained zones from arrested dentin caries lesions described here indicates different mechanical properties and microstructure between and among zones, which is valuable for caries diagnosis. However, analysis of our data suggests that the pink zone, which is commonly removed by the clinician, could contain residual mineral, and thus may be worth retaining.

ACKNOWLEDGMENTS

The authors acknowledge G. Nonomura for tooth collection and support from NIH/NIDCR grants T32 DE 00736, P01 DE09859, and R01 DE16849.

REFERENCES

Anderson MH, Loesche WJ, Charbeneau GT (1985). Bacteriologic study of a basic fuchsin caries-disclosing dye. *J Prosthet Dent* 54:51-55.

Angker L, Nijhof N, Swain MV, Kilpatrick NM (2004a). Influence of hydration and mechanical characterization of carious primary dentine using an ultra-micro indentation system (UMIS). *Eur J Oral Sci* 112:231-236.

Angker L, Nockolds C, Swain MV, Kilpatrick N (2004b). Correlating the mechanical properties to the mineral content of carious dentine—a comparative study using an ultra-micro indentation system (UMIS) and SEM-BSE signals. *Arch Oral Biol* 49:369-378.

Arends J, ten Bosch JJ (1992). Demineralization and remineralization evaluation techniques. *J Dent Res* 71(Spec Iss):924-928.

Balooch M, Wu-Magidi IC, Lundkvist AS, Balazs A, Marshall SJ, Marshall GW, *et al*. (1998). Viscoelastic properties of demineralized human dentin in water with AFM-based indentation. *J Biomed Mater Res* 40:539-544.

Bonar LC, Lees S, Mook HA (1985). Neutron diffraction studies of collagen in fully mineralized bone. *J Mol Biol* 181:265-270.

Darling CL, Huynh GD, Fried D (2006). Light scattering properties of natural and artificially demineralized dental enamel at 1310 nm. *J Biomed Opt* 11:34023, 1-11.

Doerner MF, Nix WD (1986). A method for interpreting the data from depth-sensing indentation instruments. *J Mater Res* 1:601-609.

Featherstone JD (2004). The caries balance: the basis for caries management by risk assessment. *Oral Health Prev Dent* 2(Suppl 1):259-264.

Featherstone JD, ten Cate JM, Shariati M, Arends J (1983). Comparison of artificial caries-like lesions by quantitative microradiography and microhardness profiles. *Caries Res* 17:385-391.

Featherstone JD, Glena R, Shariati M, Shields CP (1990). Dependence of *in vitro* demineralization of apatite and remineralization of dental enamel on fluoride concentration. *J Dent Res* 69(Spec Iss):620-625.

Fusayama T (1991). Intratubular crystal deposition and remineralization of carious dentin. *J Biol Buccale* 19:255-262.

Fusayama T, Terachima S (1972). Differentiation of two layers of carious dentin by staining. *J Dent Res* 51:866.

Habelitz S, Marshall GW Jr, Balooch M, Marshall SJ (2002). Nanoindentation and storage of teeth. *J Biomech* 35:995-998.

Kidd EA, Joyston-Bechal S, Beighton D (1993). Microbiological validation of assessments of caries activity during cavity preparation. *Caries Res* 27:402-408.

Kinney JH, Balooch M, Marshall GW, Marshall SJ (1993). Atomic-force microscopic study of dimensional changes in human dentine during drying. *Arch Oral Biol* 38:1003-1007.

Kinney JH, Balooch M, Marshall SJ, Marshall GW Jr, Weihs TP (1996). Hardness and Young's modulus of human peritubular and intertubular dentine. *Arch Oral Biol* 41:9-13.

Kinney JH, Habelitz S, Marshall SJ, Marshall GW (2003). The importance of intrafibrillar mineralization of collagen on the mechanical properties of dentin. *J Dent Res* 82:957-961.

Kodaka T, Debari K, Yamada M, Kuroiwa M (1992). Correlation between microhardness and mineral content in sound human enamel (short communication). *Caries Res* 26:139-141.

Kuboki Y, Ohgushi K, Fusayama T (1977). Collagen biochemistry of the two layers of carious dentin. *J Dent Res* 56:1233-1237.

Kuboki Y, Liu CF, Fusayama T (1983). Mechanism of differential staining in carious dentin. *J Dent Res* 62:713-714.

Landis WJ, Hodgens KJ, Arena J, Song MJ, McEwen BF (1996). Structural relations between collagen and mineral in bone as determined by high voltage electron microscopic tomography. *Microsc Res Tech* 33: 192-202.

Marshall GW Jr (1993). Dentin: microstructure and characterization. *Quintessence Int* 24:606-617.

Marshall GW Jr, Wu-Magidi IC, Watanabe LG, Inai N, Balooch M, Kinney JH, *et al.* (1998). Effect of citric acid concentration on dentin demineralization, dehydration, and rehydration: atomic force microscopy study. *J Biomed Mater Res* 42:500-507.

Marshall GW, Habelitz S, Gallagher R, Balooch M, Balooch G, Marshall SJ (2001). Nanomechanical properties of hydrated carious human dentin. *J Dent Res* 80:1768-1771.

Marshall GW, Marshall SJ, Balooch M, Kinney JH (2004). Evaluating demineralization and mechanical properties of human dentin with AFM. *Methods Molec Biol* 242:141-159.

McComb D (2000). Caries-detector dyes—how accurate and useful are they? *J Can Dent Assoc* 66:195-198.

Ohgushi K, Fusayama T (1975). Electron microscopic structure of the two layers of carious dentin. *J Dent Res* 54:1019-1026.

Oliveira SS, Pugach MK, Hilton JF, Watanabe LG, Marshall SJ, Marshall GW Jr (2003). The influence of the dentin smear layer on adhesion: a self-etching primer vs. a total-etch system. *Dent Mater* 19:758-767.

Oliver WC, Pharr GM (1992). An improved technique for determining hardness and elastic modulus using load and displacement sensing indentation experiments. *J Mater Res* 7:1564-1583.

ten Cate JM, Timmer K, Shariati M, Featherstone JD (1988). Effect of timing of fluoride treatment on enamel de- and remineralization in vitro: a pH-cycling study. *Caries Res* 22:20-26.

White JM, Goodis HE, Marshall SJ, Marshall GW (1994). Sterilization of teeth by gamma radiation. *J Dent Res* 73:1560-1567.

Zacharia MA, Munshi AK (1995). Microbiological assessment of dentin stained with a caries detector dye. *J Clin Pediatr Dent* 19:111-115.

Zheng L, Hilton JF, Habelitz S, Marshall SJ, Marshall GW (2003). Dentin caries activity status related to hardness and elasticity. *Eur J Oral Sci* 111:243-252.